Mathematical Modelling and Numerical Simulation with Applications, 2021, 1(2), 84–94

https://www.mmnsa.org
ISSN Online: 2791-8564 / Open Access
https://doi.org/10.53391/mmnsa.2021.01.008

RESEARCH PAPER

Chaos of calcium diffusion in Parkinson's infectious disease model and treatment mechanism via Hilfer fractional derivative

Hardik Joshi[1,*,†,‡] and Brajesh Kumar Jha[2,†,‡]

[1]Department of Mathematics, LJ Institute of Engineering and Technology, LJ University, Ahmedabad-382210, Gujarat, India , [2]Department of Mathematics, School of Technology, Pandit Deendayal Energy University, Gandhinagar-382007, Gujarat, India

*Corresponding Author
†hardik.joshi8185@gmail.com (Hardik Joshi); brajeshjha2881@gmail.com (Brajesh Kumar Jha)
‡Contributed equally.

Abstract

Calcium is a vital element in our body and plays a crucial role to moderate the calcium signalling process. Calcium-dependent protein and flux through the sodium-calcium exchanger are also involved in signalling process to perform and execute necessary cellular activities. The loss or alteration in this cellular activity starts the early progress of Parkinson's disease. A mathematical calcium model is developed in the form of the Hilfer fractional reaction-diffusion equation to examine the calcium diffusion in the cells. The effect of calcium-dependent protein and flux through the sodium-calcium exchanger is incorporated in the model. The solution of the Hilfer fractional calcium model is obtained by using the Sumudu transform technique in the form of the Wright function and Mittag-Leffler function. The graphical results are obtained for the different amounts of proteins, presence, and absence of sodium-calcium exchanger, and various orders of Hilfer derivative. The obtained results show that the modified calcium model is a function of time, position, and Hilfer fractional derivative. Thus the modified Hilfer calcium model provides a rich physical interpretation of a calcium model as compared to the classical calcium model.

Key words: Calcium; sodium-calcium exchanger; Parkinson's disease; Hilfer fractional derivative; Sumudu transform
AMS 2020 Classification: 26A33; 35Q92; 35R11; 92B05

1 Introduction

Neurons a main component of the brain also refer as nerve cells that transfer the message from the brain to other parts in the form of electrochemical gradient and vice versa. The major part of a neuron is made by a combination of a cell body, axon, and dendrite. Dendrite is a long tree like structure that receives information from the other neurons and is passed to the cell body. The cell body is a central part of the neuron that analyzed the received information and prepared a necessary outcome. The axon received the outcomes and carries them to other neurons. This is the basic life cycle of a typical neuron. Our brain consists of around 80-90 billion neurons so it made a complex neuronal network to perform and execute cellular activities [1]. Besides neuron, astrocytes and glial cells are also supports and moderate the requisite cellular activities [2].

Calcium is also known as the second messenger and it is found in almost all kinds of nerve cells such as a neuron, astrocytes, oocytes, and many others. Calcium diffusion is a very dynamic process in the cells to understand the calcium signalling phenomena. Calcium diffuses

➤ **Received:** 06.11.2021 ➤ **Revised:** 06.12.2021 ➤ **Accepted:** 07.12.2021 ➤ **Published:** 16.12.2021

into the cell and reacts with protein, channels, pumps, and many other cellular entities. Due to the complexity, we have incorporated the flux through a sodium calcium exchanger in the presence of protein only. They diffused and produce the calcium depending protein as per a requirement of the calcium signalling process. The cytosol feels like a full of free calcium then the calcium buffering phenomena convert the level of free calcium into calcium dependent protein. That generated protein is utilized for fertilization, cell differentiation, synaptogenesis, and so on [3, 4]. The sodium calcium exchanger is also one of the major sources to transform free calcium from the cytosol to cells. They exchange three sodium ions against one calcium ion. That is three sodium ions enter into the cytosol and one calcium ion exists from the cytosol. In the present study, we have considered the sodium calcium exchanger with an exchange ratio of $3Na^{+} : 1Ca^{++}$ [5, 6, 7]. The alteration in the process to manage free calcium in the cells for long periods may result in various neurological diseases namely Parkinson's, Alzheimer's, Amyotrophic lateral sclerosis, etc [8, 9]. Parkinson's disease (PD) is a disorder of the nervous system strongly associated with the dysfunction or alteration of calcium signalling. There is numerous factor associated with it such as environmental effect, age, gene mutation, misfolded protein sequence, calcium homeostasis, etc [10, 11, 12].

Panday and Pardasani have employed the finite element method to study the role of sodium calcium exchanger on calcium diffusion in oocytes cells [5]. Tewari and Pardasani have employed Gear's method to study the role of sodium calcium exchanger, calcium channel, plasma membrane, sodium pump and buffer on calcium diffusion in neuron cells [6]. Jha et al. have employed the finite element method to study the role of sodium calcium exchanger by considering a point source and line source of calcium flux on calcium diffusion in neuron cells [7]. Also, there have been several experimental attempts that were performed in the past to identify the role and physiological impact of sodium calcium exchangers on various cells [13, 14, 15, 16]. Beside this a researches has explored the role of parameters of calcium toolkits on astrocytes [17, 18, 19, 20, 21, 22], neuron [23, 24, 25, 26, 27, 28, 29, 30], oocytes [31, 32], myocytes [33, 34, 35], hepatocytes [36], and *T* lymphocytes cells [37, 38]. Thus a very little amount of work has attempted to study parameters of calcium toolkits by using the fractional calculus approach. Also, the literature suggests that none of the researchers and scientists has studied the effect of sodium calcium exchanger and protein on calcium diffusion and related to Parkinson's disease. Therefore, in this paper, we have studied the role of sodium calcium exchanger and calcium dependent protein on calcium diffusion by using the fractional calculus approach.

The fractional calculus is a generalization of the integer-order calculus and it provides more accurate results as compared to classical calculus. Hence, it is widely used in mathematical modelling of science and engineering, medical, and almost all area of education [39, 40, 41, 42, 43, 44, 45, 46, 47, 48, 49, 50, 51, 52, 53, 54, 55, 56, 57, 58, 59, 60]. Nowadays, numbers of the fractional derivative are available to deal with real-world problems such as Caputo derivative, Caputo-Fabrizio derivative, Atangana-Baleneu derivative, Hilfer derivative, Weyl derivative, Conformable derivative and many more. We have used the Hilfer fractional derivative in this study because it is a generalization of the Caputo and Riemann-Liouville derivatives [61]. Also, there are a number of effective methods such as differential transform method, double Laplace transform, Fourier transform method, Sumudu transform method, iterative method, Adomian decomposition method, homotopy transform method, and many more. We have used the Sumudu transform method in this study because it is best to our problems and it provides a closed form solution of the calcium model in terms of Wright function and Mittag-Leffler function.

The structure of this study is as follows. In Section 2, we provide some basic definitions that are used in this study. In Section 3, we develop a mathematical formulation of the calcium model then, we modify the model in the sense of the Hilfer fractional calcium model. The results are obtained in Section 4 for different amounts of calcium protein and sodium calcium exchanger. In the last Section 5, some conclusions are derived from the proposed results.

2 Mathematical preliminaries

The mathematical model developed in the present study is solved by using the Hilfer fractional derivative and Sumudu transform technique. The basic definitions of the Hilfer derivative and Sumudu transform are provided here that can be used to solve the model [61, 62, 63, 64].

Definition 1 *The Riemann-Liouville fractional order integral for a function $y(t)$ is defined as*

$$I_a^u(y(t)) = \frac{1}{\Gamma(u)} \int_a^t (t-\xi)^{u-1} y(\xi) d\xi, \tag{1}$$

where $t > a$, and $R(u) > 0$.

Definition 2 *The Riemann-Liouville fractional order derivative for a function $y(t)$ of order u is defined as*

$${}_a^{RL}D_t^u(y(t)) = \left(\frac{d}{dt}\right)^n (I_a^{n-u} y(t)), \tag{2}$$

where $R(u) > 0$.

Definition 3 *The Caputo fractional order derivative for a function $y(t)$ of order u is defined as*

$${}_a^{C}D_t^u(y(t)) = \begin{cases} \frac{1}{\Gamma(m-u)} \int_a^t \frac{y^m(\xi)}{(t-\xi)^{u+1-m}} d\xi, & m-1 < u \le m, \\ \frac{d^m}{dt^m} y(t), & u = m, \end{cases} \tag{3}$$

where $R(u) > 0$ and $m \in N$.

Definition 4 *The Hilfer fractional derivative for a function $y(t)$ is defined as*

$$ {}^{H}_{a}D^{u,v}_{t}(y(t)) = I^{v(1-u)}_{t}\frac{\partial}{\partial t}(I^{(1-v)(1-u)}_{t}y(t)), 0 < u < 1, 0 \leq v \leq 1. \tag{4}$$

Remark 1 *The Hilfer fractional derivative is a generalization of the Riemann-Liouville and Caputo fractional definition. The Riemann-Liouville and Caputo fractional definitions are recovered by setting $v = 0$ and $v = 1$ respectively in equation (4).*

Definition 5 *Let consider a set A over the function $y(t)$ as*

$$ A = \{y(t) : \exists M, \tau_1, \tau_2 > 0, |y(t)| < Me^{t/\tau_j}, t \in (-1)^j \times [0, \infty)\}, \tag{5}$$

then the Sumudu transform of function $y(t)$ over the set A is defined as

$$ S\{y(t)\} = Y(p) = \int_0^\infty \frac{1}{p}e^{-\frac{t}{p}}y(t)dt, p \in (-\tau_1, \tau_2). \tag{6}$$

Definition 6 *The inverse Sumudu transform of function $Y(p)$ is defined as follows*

$$ S^{-1}\{Y(p)\} = y(t) = \frac{1}{2\pi i}\int_{\gamma-i\infty}^{\gamma+i\infty} e^{\frac{t}{p}}Y(p)dp, \tag{7}$$

where $\gamma \in R$ is a fixed number.

3 Mathematical formulation of the calcium model

The calcium in the cytosol is diffuse with protein and produces a different chemical species that modulate the cellular process and is represented by the chemical equation as

$$ Ca^{2+} + B_i \underset{k^-}{\overset{k^+}{\leftrightarrow}} CaB_i, \tag{8}$$

where Ca^{2+} represents calcium ion, B_i represents the proteins calbindin-D_{28k}, and CaB_i represents the produced calcium dependent protein.

The calcium flow in the cell at any position and time is determined by the following partial differential equation [23, 31, 32, 33]

$$ \frac{\partial}{\partial t}[Ca^{2+}] = D_{Ca}\frac{\partial^2}{\partial x^2}[Ca^{2+}] + \sum_i R_i + f. \tag{9}$$

The rate of change of calcium is denoted by the first order derivative with time, the diffusion of calcium is denoted by the Laplacian operator, D_{Ca} is the diffusion coefficient, f denoted the calcium source from cellular entities, whereas the summation corresponds to multiple proteins and reaction term is a combination of chemical reactant and it is described as

$$ R_i = -k^+[B_i][Ca^{2+}] + k^-[CaB_i]. \tag{10}$$

The similar chemical reaction for the proteins and calcium dependent protein follows the Fickian diffusion mechanism and is defined as [65, 66]

$$ \frac{\partial}{\partial t}[B_i] = D_B \cdot \frac{\partial^2}{\partial x^2}[B_i] + R_i, \tag{11}$$

$$ \frac{\partial}{\partial t}[CaB_i] = D_{CaB_i} \cdot \frac{\partial^2}{\partial x^2}[CaB_i] - R_i, \tag{12}$$

where D_B and D_{CaB_i} represent a diffusion coefficient of proteins and calcium dependent protein, respectively.

Thus to identify the calcium flow in the cell at any moment it is necessary to solve the given system of partial differential equation

$$ \begin{aligned} &\tfrac{\partial}{\partial t}[Ca^{2+}] = D_{Ca}\tfrac{\partial^2}{\partial x^2}[Ca^{2+}] + \textstyle\sum_i R_i + f, \\ &\tfrac{\partial}{\partial t}[B_i] = D_B \cdot \tfrac{\partial^2}{\partial x^2}[B_i] + R_i, \\ &\tfrac{\partial}{\partial t}[CaB_i] = D_{CaB_i} \cdot \tfrac{\partial^2}{\partial x^2}[CaB_i] - R_i. \end{aligned} \tag{13}$$

Modified calcium model in form of Hilfer fractional derivative

The classical model is replaced by Hilfer fractional model to catch the memory of cells that increase the complexity of a model but simultaneously increase the accuracy of a model. The classical calcium model (13) become as

$$\begin{aligned} {}_0^H D_t^{\alpha,\beta}[Ca^{2+}](x,t) &= D_{Ca}\frac{\partial^2}{\partial x^2}[Ca^{2+}](x,t) + \sum_i R_i + f(x,t),\\ {}_0^H D_t^{\alpha,\beta}[B_i](x,t) &= D_B \cdot \frac{\partial^2}{\partial x^2}[B_i](x,t) + R_i(x,t),\\ {}_0^H D_t^{\alpha,\beta}[CaB_i](x,t) &= D_{CaB_i} \cdot \frac{\partial^2}{\partial x^2}[CaB_i](x,t) - R_i(x,t), \end{aligned} \tag{14}$$

where $0 < \alpha < 1, 0 \leq \beta \leq 1$.

The molecular weight of calcium is very small as compared to proteins and calcium dependent proteins. Hence by using this assumption we have $D_B = D_{CaB_i} = D_i$ and we get the following equation

$${}_0^H D_t^{\alpha,\beta}[B_i]_T(x,t) = D_i\frac{\partial^2}{\partial x^2}[B_i]_T(x,t), \tag{15}$$

where $[B_i]_T = [B_i] + [CaB_i]$.

The background concentration of proteins and calcium dependent protein in the terms of a total concentration and dissociate constant are given as [66]

$$[B_i]_\infty = \frac{K[B_i]_T}{K + [Ca^{2+}]_\infty}, \tag{16}$$

and

$$[CaB_i]_\infty = \frac{[Ca^{2+}]_\infty[B_i]_T}{K + [Ca^{2+}]_\infty}, \tag{17}$$

where $K = k^-/k^+$.

Thus by combining equations (15-17) the model (14) is converted to a Hilfer fractional reaction diffusion equation which is given as

$${}_0^H D_t^{\alpha,\beta}[Ca^{2+}](x,t) = D_{Ca}\frac{\partial^2}{\partial x^2}[Ca^{2+}](x,t) - \sum_i k_i^+[B_i]_\infty([Ca^{2+}](x,t) - [Ca^{2+}]_\infty) + f(x,t), \tag{18}$$

where $0 < \alpha < 1, 0 \leq \beta \leq 1$.

The sodium calcium exchanger flux is considered in the model whose electrochemical gradient is involved in the signalling phenomena. There are two valence ions of calcium they provide the given equation [5, 6, 7]

$$\Delta\mu_{Ca} = ZFV_m + RT\ln\left(\frac{Ca_i}{Ca_o}\right). \tag{19}$$

Similarly, there is one valence ion of sodium they generate the following equation as a result of electrochemical gradient as

$$\Delta\mu_{Na} = ZFV_m + RT\ln\left(\frac{Na_i}{Na_o}\right). \tag{20}$$

The exchange ratio of sodium and calcium ion is 3:1 that is three sodium ions enter into the cytosol and one calcium ion removed from the cytosol. The mathematical expression of the sodium calcium exchange ratio is given as

$$3\Delta\mu_{Na} = 1\Delta\mu_{Ca}. \tag{21}$$

By combining the electrochemical gradient and sodium calcium exchange ratio the equation (19-21) becomes as

$$2FV_m + RT\ln\left(\frac{Ca_i}{Ca_o}\right) = 3FV_m + 3RT\ln\left(\frac{Na_i}{Na_o}\right). \tag{22}$$

The rearrangement of equation (22) gives us the following equation

$$\frac{Ca_i}{Ca_o} = \left(\frac{Na_i}{Na_o}\right)^3 e^{\frac{FV_m}{RT}}. \tag{23}$$

Thus the mathematical expression for the sodium calcium flux becomes

$$f_{NCX} = Ca_o\left(\frac{Na_i}{Na_o}\right)^3 e^{\frac{FV_m}{RT}}, \tag{24}$$

where Ca_i, Ca_o, Na_i and Na_o are the intracellular and extracellular flux from the respective ions. By incorporating the flux through sodium calcium exchanger into the model the equation (18) becomes

$$ {}_0^H D_t^{\alpha,\beta}[Ca^{2+}](x,t) = D_{Ca}\frac{\partial^2}{\partial x^2}[Ca^{2+}](x,t) - \sum_i k_i^+[B_i]_\infty([Ca^{2+}](x,t) - [Ca^{2+}]_\infty) - f_{NCX}. \tag{25} $$

The initial and boundary conditions of a problem are as

$$ \lim_{x\to 0}\left(-D_{Ca}\frac{\partial}{\partial x}[Ca^{2+}]\right) = \sigma_{Ca}, t > 0, \tag{26} $$

$$ \lim_{x\to\infty}\left([Ca^{2+}]\right) = [Ca^{2+}]_\infty, t \geq 0, \tag{27} $$

$$ [Ca^{2+}]\Big|_{t=0} = 0, 0 \leq x < \infty. \tag{28} $$

For sake of simplicity the equation (25) rewritten as

$$ {}_0^H D_t^{\alpha,\beta}C(x,t) = D_{Ca}\frac{\partial^2}{\partial x^2}C(x,t) - \xi\cdot C(x,t) + \psi, \tag{29} $$

where $0 < \alpha < 1, 0 \leq \beta \leq 1, \xi = k^+[B_i]_\infty$, and $\psi = k^+[B_i]_\infty C_\infty - Ca_o\left(\frac{Na_i}{Na_o}\right)^3 e^{\frac{FVm}{RT}}$.

The corresponding initial and boundary condition are

$$ \lim_{x\to 0}\left(\frac{\partial C}{\partial x}\right) = -\frac{\sigma_{Ca}}{D_{Ca}}, t > 0, \tag{30} $$

$$ \lim_{x\to\infty} C(x,t) = C_\infty, t \geq 0, \tag{31} $$

$$ C(x,0) = 0, 0 \leq x < \infty. \tag{32} $$

Applying Sumudu transform on both sides of equation (29) with respect to time then we get

$$ s^{-\alpha}\bar{C}(x,s) - s^{-1+\beta(1-\alpha)}\sum_{k=0}^{0}\frac{\partial^k}{\partial x^k}\left(I_0^{(1-\beta)(1-\alpha)}C(x,0)\right) = D_{Ca}\frac{\partial^2}{\partial x^2}\bar{C}(x,s) - \xi\cdot\bar{C}(x,s) + \psi, \tag{33} $$

Using the initial condition (32), equation (33) can be written as

$$ s^{-\alpha}\bar{C}(x,s) = D_{Ca}\frac{\partial^2}{\partial x^2}\bar{C}(x,s) - \xi\cdot\bar{C}(x,s) + \psi, \tag{34} $$

The equation (34) can be rewritten as

$$ \frac{\partial^2}{\partial x^2}\bar{C}(x,s) - \frac{1}{D_{Ca}}\left(s^{-\alpha}\bar{C}(x,s) - \xi\cdot\bar{C}(x,s) + \psi\right) = 0, \tag{35} $$

Further simplification of equation (35) lead us to the given equation

$$ \frac{\partial^2}{\partial x^2}\bar{C}(x,s) - \frac{s^{-\alpha}-\xi}{D_{Ca}}\bar{C}(x,s) - \frac{\psi}{D_{Ca}} = 0, \tag{36} $$

Thus the Sumudu transform of the equation (29) is obtained as

$$ \bar{C}(x,s) = C_1\exp\left(\sqrt{\frac{s^{-\alpha}-\xi}{D_{Ca}}}\right)x + C_2\exp\left(-\sqrt{\frac{s^{-\alpha}-\xi}{D_{Ca}}}\right)x - \frac{\psi}{s^{-\alpha}-\xi}, \tag{37} $$

By Applying the Sumudu transform on the boundary conditions (30-31), we get

$$ \frac{\partial}{\partial x}\bar{C}(0,s) = -\frac{\sigma_{Ca}}{D_{Ca}}, \tag{38} $$

and

$$\lim_{x\to\infty} \tilde{C}(x,s) = 0. \tag{39}$$

By using equations (38-39), equation (37) turns out to be

$$\tilde{C}(x,s) = \frac{\sigma_{Ca}}{\sqrt{D_{Ca}}} s^{\alpha/2} \exp\left(-\sqrt{\frac{s^{-\alpha}-\xi}{D_{Ca}}}\right) x - \frac{\psi}{s^{-\alpha}-\xi}, \tag{40}$$

To invert the Sumudu transform of equation (40) we use the following inequalities [64]

$$S^{-1}\left(p^{\alpha/2} e^{-\lambda p^{-\alpha/2}}\right) = t^{\alpha/2} W\left(-\frac{\alpha}{2}, \frac{\alpha}{2}+1, -\lambda t^{-\alpha/2}\right), \tag{41}$$

and

$$S^{-1}\left(\frac{p^{\beta-1}}{1-\lambda p^{\alpha}}\right) = t^{\beta-1} E_{\alpha,\beta}(\lambda t^{\alpha}), \tag{42}$$

By using equations (41-42) the inverse Sumudu transform of equation (40) gives the following results

$$C(x,t) = \frac{\sigma_{Ca}}{\sqrt{D_{Ca}}} e^{\sqrt{\frac{\xi}{D_{Ca}}}} t^{\alpha/2} W\left(-\frac{\alpha}{2}, \frac{\alpha}{2}+1, -\frac{x}{\sqrt{D_{Ca}}} t^{-\alpha/2}\right) - \psi t^{\alpha} E_{\alpha,\alpha+1}(\xi t^{\alpha}), \tag{43}$$

where $W(\alpha, \beta, \gamma)$ and $E_{\alpha,\beta}(z)$ are the Wright function and Mittag-Leffler function for two parameters respectively [61, 62, 63].

4 Results and discussion

The numerical values for the physical parameters are given in Table 1 and are used in the computation of the calcium profile.

Table 1. Values of physical parameters [5, 6, 7, 66]

Parameters	Values of parameters
Diffusion coefficient (D_{Ca})	200-300 ($\mu m^2/s$)
Buffer associate rate (k^+)	75 ($\mu M^{-1}s^{-1}$)
Concentration of protein ($[B_i]_\infty$)	100-360 (μM)
Intracellular sodium ($[Na^+])_i$	12 (mM)
Extracellular sodium ($[Na^+])_o$	145 (mM)
Intracellular calcium ($[Ca^{2+}])_i$	0.1 (μM)
Extracellular calcium ($[Ca^{2+}])_o$	1.8 (mM)
Source amplitude of calcium (σ_{Ca})	1.4 ($\mu M^{-1}s^{-1}$)
Faraday's constant (F)	96485 (C/mol)
Gas constant (R)	8.314 (J)
Temperature (T)	310 (^oK)
Membrane potential (V_m)	-0.06 (V)

The solution (43) of the modified calcium model (14) in form of Hilfer fractional derivative is used to obtain a graphical calcium profile for low and high proteins level and sodium calcium exchanger. The calcium profile simulated for the values $D_{Ca} = 250\mu m^2/s$, low protein level $[B_i]_\infty = 120\mu M$, high protein level $[B_i]_\infty = 340\mu M$ and for various values of α in Figures 1 to 6. Figures 1-3 show variations of calcium versus time for different biophysical parameters whereas Figures 4-6 show variations of calcium versus position for different biophysical parameters.

In Figure 1 we show calcium profile versus time near the source $x = 0$ for the low level of proteins level and presence of sodium calcium exchanger. The calcium profile is high for the lower values of fractional order up to 0.35 seconds then the calcium profile is high for the higher values of α and after 0.7 seconds the calcium profile achieves the steady level.

Figure 2 shows calcium profile versus time near the source $x = 0$ for a high level of proteins and presence of sodium calcium exchanger. The profile suddenly attains the peak near 0.1 second due to high level of proteins then decrease gradually to attain a steady level. The peak level of calcium profile in figure 2 is less compared to figure 1. This happened due to high proteins reacting with calcium in cytosol and producing calcium dependent protein that reduce the peak values of calcium profile and protect the neuron cells from the high level of calcium. A high level of calcium for large periods is toxic for cells and generates the symptoms of Parkinson's disease.

Figure 3 represents the calcium profile versus time for the low level of proteins level and absence of sodium calcium exchanger. The profile gradually rise and achieved a peak value due to low protein level. The profile attains more peak values as compared to Figure 1 due to the absence of sodium calcium exchanger as it removed the calcium from the cells against sodium. Thus the presence of sodium calcium

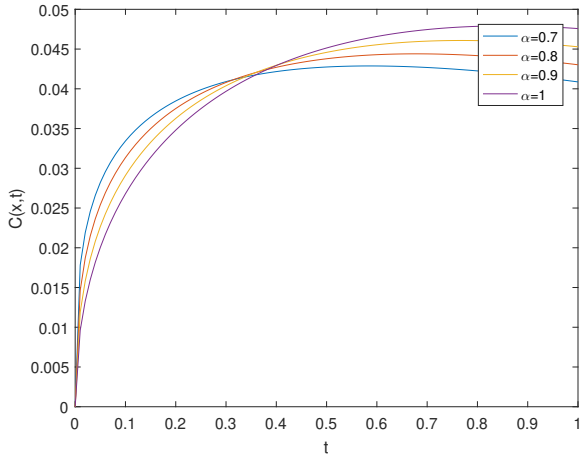

Figure 1. Calcium profile versus time for low amount of proteins at different values of α

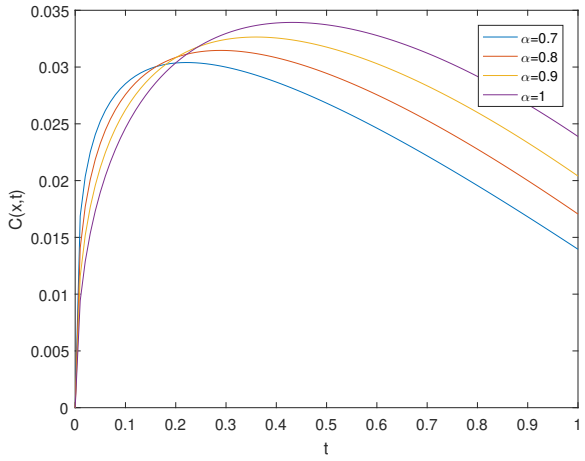

Figure 2. Calcium profile versus time for high amount of proteins at different values of α

exchanger plays a significant role in the presence of low proteins as high protein level reduces the significance of sodium calcium exchanger.

In Figure 4 we show calcium profile versus position for a $t = 0.5$ second at low proteins level and presence of sodium calcium exchanger. The calcium profile is high at the mouth of channels and slowly decrease as the position is increased. The profile is high for large values of α in the cells as the fractional order decreases the calcium profile also decreases and attains a steady level.

Figure 5 shows calcium profile versus position at $t = 0.5$ second for high proteins level and presence of sodium calcium exchanger. The profile is high at the mouth of the channel due to the high level of proteins then decreasing gradually to attain a steady level. The peak level of calcium profile in figure 5 is less compared to figure 4. The physiological results for this are the same as given in figure 2 that is high level proteins react with calcium and produce calcium protein that reduces the calcium profile and protect the cells from toxic level and symptoms of Parkinson's disease.

Figure 6 shows calcium profile versus position for low proteins level and absence of sodium calcium exchanger. The profile is at a peak level at the beginning due to the absence of sodium calcium exchanger as it did not remove the free calcium from the cells. The absence of sodium calcium exchanger and low proteins level results in an elevation in the calcium profile. It is observed that the sodium calcium exchanger is a good source of calcium flux to control the free calcium level in the cells and ultimately protect cells against Parkinson's disease.

The obtained results (43) show that the modified calcium model (14) is a function of time, position and Hilfer fractional derivative. Also, the graphical results show that the modified Hilfer calcium model provides a rich physical interpretation of a calcium model as compared to the classical calcium model.

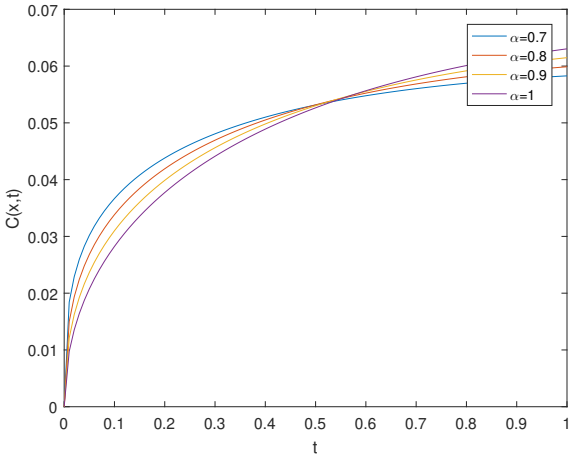

Figure 3. Calcium profile versus time for low amount of proteins and in absence of sodium calcium exchanger at different values of α

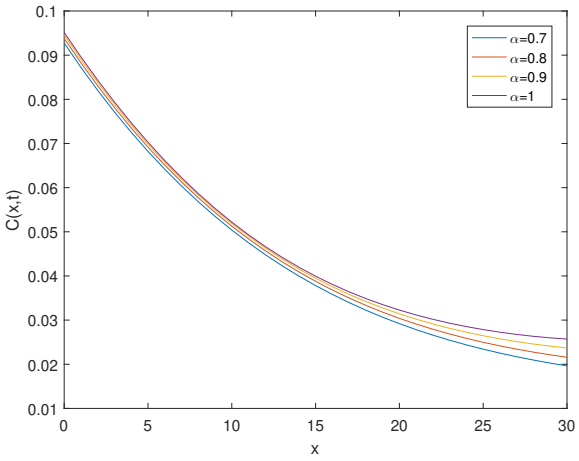

Figure 4. Calcium profile versus position for low amount of proteins at different values of α

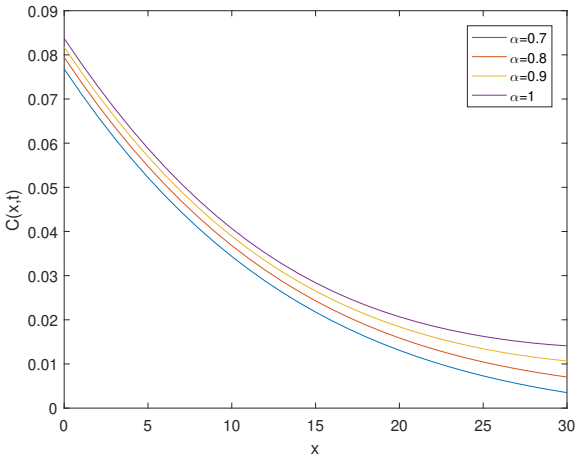

Figure 5. Calcium profile versus position for high amount of proteins at different values of α

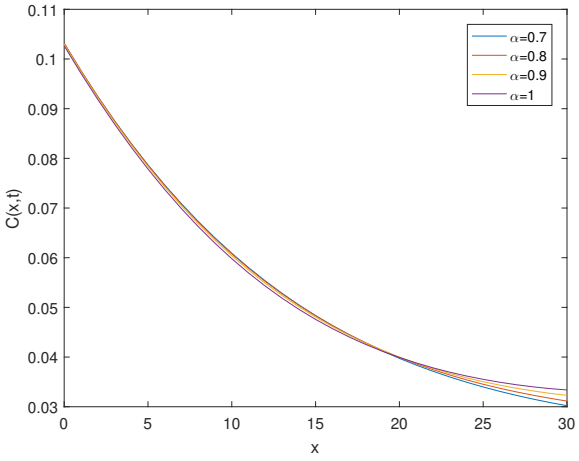

Figure 6. Calcium profile versus position for low amount of proteins and in absence of sodium calcium exchanger at different values of α

5 Conclusion

Hilfer fractional calcium model is a novel modification of the classical calcium model for neuron cells. We developed a Hilfer fractional calcium model to examine the role of calcium dependent protein, sodium calcium exchanger on calcium diffusion and related to Parkinson's disease. We obtained a closed form solution of the calcium model in the terms of Wright function and Mittag-Leffler function by using the Sumudu transform technique and Hilfer fractional derivative. High level proteins react with the calcium in cytosol and produce calcium dependent proteins that reduce the peak values of calcium profile and protect the neuron cells from the high level of calcium. A high level of calcium for large periods is toxic for cells and generates the symptoms of Parkinson's disease. The significant effect of sodium calcium exchanger has been observed for the low level of calcium dependent protein. The calcium dependent protein and sodium calcium exchanger play a crucial role to control the calcium level in the cytosol. Thus the amalgamation of the calcium dependent protein and sodium calcium exchanger control the calcium level and provide protection to neuron cell from the toxicity produced by the Parkinsonic cells. Thus Hilfer calcium model provides a rich physical interpretation of a calcium model as compared to the classical calcium model. The present model can be extended by considering the flux through various calcium channels, pumps, and receptors. A novel fractional model will be developed by considering the flux through all these parameters and expresses the obtained results with Parkinson's disease.

Declarations

Consent for publication

Not applicable.

Conflicts of interest

The authors declare that they have no conflict of interests.

Funding

Not applicable.

Author's contributions

H.J.: Conceptualization, Methodology, Investigation, Visualization, Writing, Software, Original draft preparation, Validation, Writing-Reviewing and Editing. B.K.J.: Conceptualization, Supervision, Validation, Writing-Reviewing and Editing. All authors discussed the results and contributed to the final manuscript.

Acknowledgements

The authors would like to thank the editor and reviewers for their fruitful comments and suggestions that improve the quality of the manuscript.

References

[1] Squire L.R., Berg D., Bloom F. E., Du Lac S., Ghosh A., and Spitzer N. C., *Fundamental Neuroscience*, (Vol. 4). Elsevier Inc., (2012).
[2] Verkhratsky A. & Butt A. *Glial neurobiology: a textbook*, John Wiley and Sons, (2007).

[3] Petersen, O.H., Michalak, M. & Verkhratsky A. Calcium signalling: past, present and future. *Cell Calcium*, 38(3-4), 161–169, (2005). [CrossRef]
[4] Clapham, D.E. Calcium Signaling. *Cell*, 131(6), 1047–1058, (2007). [CrossRef]
[5] Panday, S. & Pardasani, K.R. Finite element model to study effect of advection diffusion and Na +/Ca2+ exchanger on Ca2+ distribution in oocytes. *Journal of Medical Imaging and Health Informatics*, 3(3), 374–379, (2013). [CrossRef]
[6] Tewari, S.G. & Pardasani, K.R. Modeling effect of sodium pump on calcium oscillations in neuron cells. *Journal of Multiscale Modelling*, 4(3), 1250010, (2012). [CrossRef]
[7] Jha, A., Adlakha, N. & Jha, B.K. Finite element model to study effect of Na+ - Ca2+ exchangers and source geometry on calcium dynamics in a neuron cell. *Journal of Mechanics in Medicine and Biology*, 16(2), 1–22, (2015). [CrossRef]
[8] Mattson, M.P. Calcium and neurodegeneration. *Aging Cell*, 6(3), 337–350, (2007). [CrossRef]
[9] Bezprozvanny, I. Calcium signaling and neurodegenerative diseases. *Trends in molecular medicine*, 15(3), 89–100, (2009). [CrossRef]
[10] Surmeier, D.J. Calcium, ageing, and neuronal vulnerability in Parkinson's disease. *The Lancet Neurology*, 6(10), 933–938, (2007). [CrossRef]
[11] Zaichick, S.V., McGrath, K.M. & Caraveo, G. The role of Ca2+ signaling in Parkinson's disease. *Disease Models & Mechanisms*, 10(5), 519–535, (2017). [CrossRef]
[12] Calì, T., Ottolini, D. & Brini, M. Calcium signaling in Parkinson's disease. *Cell and tissue research*, 357(2), 439–454, (2014). [CrossRef]
[13] Blaustein, M.P. & Lederer, W.J. Sodium/calcium exchange: Its physiological implications. *Physiological Reviews*, 79(3), 763–854, (1999). [CrossRef]
[14] Sato, D., Despa, S. & Bers, D.M. Can the sodium-calcium exchanger initiate or suppress calcium sparks in cardiac myocytes? *Biophysical journal*, 102(8), L31–L33, (2012). [CrossRef]
[15] Philipson, K.D. & Nicoll, D.A. Sodium-calcium exchange: a molecular perspective. *Annual review of physiology*, 62(1), 111–133, (2000). [CrossRef]
[16] Noble, D., Noble, S.J., Bett, G.C.L., Earm, Y.E., Ho, W.K. & So, I.K. The Role of Sodium - Calcium Exchange during the Cardiac Action Potential a. *Annals of the New York Academy of Sciences*, 639(1), 334–353, (1991). [CrossRef]
[17] Jha, B.K., Adlakha, N. & Mehta, M.N. Two-Dimensional Finite Element Model To Study Calcium Distribution in Astrocytes in Presence of VGCC and Excess Buffer. *International Journal of Modeling, Simulation, and Scientific Computing*, 4(2), 1250030, (2013).
[18] Jha, B.K. & Jha, A. Two dimensional finite element estimation of calcium ions in presence of NCX and Buffers in Astrocytes. *Boletim da Sociedade Paranaense de Matemática*, 36(1), 151–160, (2018). [CrossRef]
[19] Jha, B.K., Jha, A. & Adlakha, N. Three-Dimensional Finite Element Model to Study Calcium Distribution in Astrocytes in Presence of VGCC and Excess Buffer. *Differential Equations and Dynamical Systems*, 28(3), 603–616,(2020).
[20] Jha, B.K., Adlakha, N. & Mehta, M.N. Two-dimensional finite element model to study calcium distribution in astrocytes in presence of excess buffer. *International Journal of Biomathematics*, 7(03), 1450031, (2014).
[21] Gill, V., Singh, Y., Kumar, D. & Singh, J. Analytical study for fractional Order mathematical model of concentration of Ca2+ in astrocytes cell with a composite fractional derivative. *Journal of Multiscale Modelling*, 11(3), 2050005, (2020). [CrossRef]
[22] Devi, A. & Jakhar, M. Analysis of Concentration of Ca2 + Arising in Astrocytes Cell. *International Journal of Applied and Computational Mathematics*, 7(1), 1–9, (2021). [CrossRef]
[23] Jha, A. & Adlakha, N. Two-dimensional finite element model to study unsteady state Ca2+ diffusion in neuron involving ER LEAK and SERCA. *International Journal of Biomathematics*, 8(01), 1550002, (2015). [CrossRef]
[24] Joshi, H. & Jha, B.K. Fractionally delineate the neuroprotective function of calbindin-28k in Parkinson's disease. *International Journal of Biomathematics*, 11(08), 1850103, (2018). [CrossRef]
[25] Joshi H. and Jha B. K. Generalized Diffusion Characteristics of Calcium Model with Concentration and Memory of Cells: A Spatiotemporal Approach. *Iranian Journal of Science and Technology, Transactions A: Science*, 1–14, (2021). [CrossRef]
[26] Joshi, H. & Jha, B.K. On a reaction–diffusion model for calcium dynamics in neurons with Mittag–Leffler memory. *The European Physical Journal Plus*, 136(6), 1–15, (2021). [CrossRef]
[27] Joshi, H. & Jha, B.K. Modeling the spatiotemporal intracellular calcium dynamics in nerve cell with strong memory effects. *International Journal of Nonlinear Sciences and Numerical Simulation*, (2021). [CrossRef]
[28] Joshi, H. & Jha, B.K. Fractional-order mathematical model for calcium distribution in nerve cells. *Computational and Applied Mathematics*, 39(2), 1–22, (2020). [CrossRef]
[29] Jha, B.K., Joshi, H. & Dave, D.D. Portraying the Effect of Calcium-Binding Proteins on Cytosolic Calcium Concentration Distribution Fractionally in Nerve Cells. *Interdisciplinary Sciences: Computational Life Sciences*, 10(4), 674–685, (2018). [CrossRef]
[30] Dave, D.D. & Jha, B.K. Mathematical Modeling of Calcium Oscillatory Patterns in a Neuron. *Interdisciplinary Sciences: Computational Life Sciences*, 13(1), 12–24, (2021). [CrossRef]
[31] Naik, P.A. & Pardasani, K.R. Finite element model to study calcium distribution in oocytes involving voltage gated Ca2 + channel, ryanodine receptor and buffers. *Alexandria Journal of Medicine*, 52(1), 43–49, (2016). [CrossRef]
[32] Naik, P.A. & Pardasani, K.R. Three-dimensional finite element Model to Study Effect of RyR Calcium Channel, ER Leak and SERCA Pump on calcium distribution in oocyte cell. *International Journal of Computational Methods*, 16(01), 1850091, (2019). [CrossRef]
[33] Pathak, K. & Adlakha, N. Finite element model to study two dimensional unsteady state calcium distribution in cardiac myocytes. *Alexandria Journal of Medicine*, 52(3), 261–268, (2016). [CrossRef]
[34] Chen, W., Aistrup, G., Wasserstrom J.A. & Shiferaw, Y. A mathematical model of spontaneous calcium release in cardiac myocytes. *American Journal of Physiology-Heart and Circulatory Physiology*, 300(5), H1794-H1805, (2011). [CrossRef]
[35] Singh, N. & Adlakha, N. A mathematical model for interdependent calcium and inositol 1,4,5-trisphosphate in cardiac myocyte. *Network Modeling Analysis in Health Informatics and Bioinformatics*, 8(1), 1–15, (2019). [CrossRef]
[36] Jagtap, Y. & Adlakha, N. Numerical study of one-dimensional buffered advection–diffusion of calcium and IP 3 in a hepatocyte cell. *Network Modeling Analysis in Health Informatics and Bioinformatics*, 8(1), 1–9, (2019). [CrossRef]
[37] Naik, P.A. & Zu, J. Modeling and simulation of spatial-temporal calcium distribution in T lymphocyte cell by using a reaction-diffusion equation. *Journal of bioinformatics and computational biology*, 18(2), 2050013, (2020). [CrossRef]
[38] Naik, P.A. Modeling the mechanics of calcium regulation in T lymphocyte: A finite element method approach. *International Journal of Biomathematics*, 13(05), 2050038, (2020). [CrossRef]

[39] Yavuz, M., Coşar, F.Ö., Günay F., & Özdemir, F.N. A new mathematical modeling of the COVID-19 pandemic including the vaccination campaign. *Open Journal of Modelling and Simulation*, 9(3), 299–321, (2021). [CrossRef]
[40] Özkose, F. & Yavuz M. Investigation of interactions between COVID-19 and diabetes with hereditary traits using real data: A case study in Turkey. *Computers in biology and medicine*, 105044, (2021). [CrossRef]
[41] Abboubakar, H., Kumar, P., Erturk V.S. & Kumar, A. A mathematical study of a tuberculosis model with fractional derivatives. *International Journal of Modeling, Simulation, and Scientific Computing*, 2150037, (2021). [CrossRef]
[42] Kumar, P. & Erturk, V.S. Environmental persistence influences infection dynamics for a butterfly pathogen via new generalised Caputo type fractional derivative. *Chaos, Solitons & Fractals*, 144, 110672, (2021). [CrossRef]
[43] Abboubakar, H., Kumar, P., Rangaig, N.A. & Kumar, S. A malaria model with Caputo-Fabrizio and Atangana-Baleanu derivatives. *International Journal of Modeling, Simulation, and Scientific Computing*, 12(2), 2150013, (2021). [CrossRef]
[44] Abu-Shady, M. & Kaabar, M.K. A Generalized Definition of the Fractional Derivative with Applications. *Mathematical Problems in Engineering*, 2021, (2021). [CrossRef]
[45] Debbouche, N., Ouannas, A., Batiha, I.M., Grassi, G., Kaabar, M.K., Jahanshahi, H., ... & Aljuaid, A.M. Chaotic Behavior Analysis of a New Incommensurate Fractional-Order Hopfield Neural Network System. *Complexity*, 2021, (2021). [CrossRef]
[46] Mohammadi, H., Kaabar, M.K.A, Alzabut, J., Selvam, A. & Rezapour, S. A Complete Model of Crimean-Congo Hemorrhagic Fever (CCHF) Transmission Cycle with Nonlocal Fractional Derivative. *Journal of Function Spaces*, 2021, (2021). [CrossRef]
[47] Kumar, P., Erturk, V.S., Banerjee, R., Yavuz, M. & Govindaraj, V. Fractional modeling of plankton-oxygen dynamics under climate change by the application of a recent numerical algorithm. *Physica Scripta*, 96(12), 124044, (2021). [CrossRef]
[48] Bonyah, E., Yavuz, M., Baleanu, D. & Kumar, S. A robust study on the listeriosis disease by adopting fractal-fractional operators. *Alexandria Engineering Journal*, 61(3), 2016-2028, (2021). [CrossRef]
[49] Veeresha, P. A Numerical Approach to the Coupled Atmospheric Ocean Model Using a Fractional Operator. *Mathematical Modelling and Numerical Simulation with Applications (MMNSA)*, 1(1), 1–10, (2021). [CrossRef]
[50] Erturk, V.S., Godwe, E., Baleanu, D., Kumar, P., Asad, J. & Jajarmi, A. Novel Fractional-Order Lagrangian to Describe Motion of Beam on Nanowire. *Acta Physica Polonica, A.*, 140(3), 265–272, (2021). [CrossRef]
[51] Allegretti, S., Bulai, I.M., Marino, R., Menandro, M.A. & Parisi, K. Vaccination effect conjoint to fraction of avoided contacts for a Sars-Cov-2 mathematical model. *Mathematical Modelling and Numerical Simulation with Applications (MMNSA)*, 1(2), 56–66, (2021). [CrossRef]
[52] Hammouch, Z., Yavuz, M. & Özdemir N. Numerical Solutions and Synchronization of a Variable-Order Fractional Chaotic System. *Mathematical Modelling and Numerical Simulation with Applications (MMNSA)*, 1(1), 11–23, (2021). [CrossRef]
[53] Naik, P.A., Yavuz, M., Qureshi, S., Zu, J. & Townley, S. Modeling and analysis of COVID-19 epidemics with treatment in fractional derivatives using real data from Pakistan. *The European Physical Journal Plus*, 135(10), 1-42, (2020). [CrossRef]
[54] Dasbasi, B. Stability Analysis of an Incommensurate Fractional-Order SIR Model. *Mathematical Modelling and Numerical Simulation with Applications (MMNSA)*, 1(1), 44–55, (2021). [CrossRef]
[55] Yokuş, A. Construction of Different Types of Traveling Wave Solutions of the Relativistic Wave Equation Associated with the Schrödinger Equation. *Mathematical Modelling and Numerical Simulation with Applications (MMNSA)*, 1(1), 24–31, (2021). [CrossRef]
[56] Kumar, P., Erturk, V.S., Yusuf, A. & Kumar, S. Fractional time-delay mathematical modeling of Oncolytic Virotherapy. *Chaos, Solitons & Fractals*, 150, 111123, (2021). [CrossRef]
[57] Kumar, P., Ertürk, V.S. & Nisar, K.S. Fractional dynamics of huanglongbing transmission within a citrus tree. *Mathematical Methods in the Applied Sciences*, 44(14), 11404–11424, (2021). [CrossRef]
[58] Kumar, P., Erturk, V.S., Yusuf, A., Nisar, K.S. & Abdelwahab, S.F. A study on canine distemper virus (CDV) and rabies epidemics in the red fox population via fractional derivatives. *Results in Physics*, 25, 104281, (2021). [CrossRef]
[59] Odibat, Z., Erturk, V.S., Kumar, P. & Govindaraj, V. Dynamics of generalized Caputo type delay fractional differential equations using a modified Predictor-Corrector scheme. *Physica Scripta*, 96(12), 125213, (2021). [CrossRef]
[60] Kumar, P., Erturk, V.S. & Almusawa, H. Mathematical structure of mosaic disease using microbial biostimulants via Caputo and Atangana–Baleanu derivatives. *Results in Physics*, 24, 104186, (2021). [CrossRef]
[61] Hilfer, R. *Applications of Fractional Calculus in Physics*, World Scientific: Singapore, (2000).
[62] Oldham, K.B. & Spanier, J. *The Fractional Calculus: Theory and Applications of differentiation and integration of arbitrary Order*, Elsevier, (2006).
[63] Podlubny, I. *Fractional differential equations: an introduction to fractional derivatives, fractional differential equations, to methods of their solution and some of their applications*, (Vol.1), Academic Press, Elsevier, (1998).
[64] Watugala, G.K. Sumudu transform: A new integral transform to solve differential equations and control engineering problems. *International Journal of Mathematical Education in Science and Technology*, 24(1), 35–43, (1993). [CrossRef]
[65] Crank, J. *The Mathematics of Diffusion*, (Vol.2), Oxford University Press: Oxford, (1975).
[66] Sherman, A., Smith, G.D., Dai, L. & Miura, R.M. Asymptotic analysis of buffered calcium diffusion near a point source. *SIAM Journal on Applied Mathematics*, 61(5), 1816–1838, (2001). [CrossRef]